MOUNTAIN-PLAINS CONSORTIUM

MPC 20-412 | K. Czyzyk, D. Mirossi, and J.D. Niemann

Incorporating River Network Structure for Improved Hydrologic Design of Transportation Infrastructure

A University Transportation Center sponsored by the U.S. Department of Transportation serving the Mountain-Plains Region. Consortium members:

Colorado State University
North Dakota State University
South Dakota State University
University of Colorado Denver
University of Denver
University of Utah
Utah State University
University of Wyoming

Incorporating River Network Structure for Improved Hydrologic Design of Transportation Infrastructure

Kelsey A. Czyzyk
Dario Mirossi
Jeffrey D. Niemann (PI)

Department of Civil and Environmental Engineering
Colorado State University
Fort Collins, CO 80523

March 2020

Acknowledgments

The authors thank the Mountain-Plains Consortium and Colorado State University for providing funds that made this study possible. The authors also thank Jorge Gironás for his assistance throughout the project and Almoatasem Maamon, Sediqa Hassani, Michael Coleman, and Tomas Bunster for their assistance in generating preliminary results.

ABSTRACT

When designing transportation infrastructure, stormflow hydrographs are commonly estimated using synthetic unit hydrograph (UH) methods, particularly for ungauged basins. Current synthetic UHs either consider very limited aspects of basin geometry or require explicit representation of the basin flow paths. None explicitly considers the channel network type (i.e., dendritic, parallel, pinnate, rectangular, and trellis). The goal of this study is to develop and test a nonlinear synthetic UH method that explicitly accounts for the network type. The synthetic UH is developed using kinematic wave travel time expressions for hillslope and channel points in the basin. The effects of the network structure are then isolated into two random variables whose distributions are estimated based on the network type. The proposed method is applied to 10 basins from each classification and compared with other related methods. The results suggest that considering network type improves the estimated UHs compared with neglecting it, but the classification is an adequate substitute for the individual network configuration only for pinnate basins.

TABLE OF CONTENTS

LIST OF TABLES

LIST OF FIGURES

1. INTRODUCTION

Transportation infrastructure, such as bridges and culverts, must safely convey storm flows in order to assure continued functionality and public safety. To assess the hydrologic performance of such infrastructure, consultants frequently use modeling software. Many widely used hydrologic models, such as HEC-HMS (Feldman, 2000) and SWAT (Arnold and Fohrer, 2005), represent spatial variability within a watershed using a semi-distributed approach. In this approach, the basin is divided into sub-basins (or hydrologic response units), and within each sub-basin excess rainfall (or runoff) is generated with little consideration of spatial variability. The excess rainfall is then commonly transformed into stormflow at the sub-basin outlet using a unit hydrograph (UH) method, which assumes a linear relationship between the excess rainfall and stormflow. Despite their simplicity, semi-distributed models have been shown to exhibit similar performance to fully distributed models (Abu El-Nasr et al., 2005; Haghnegahdar et al., 2015; Reed et al., 2004).

In many cases (particularly ungauged basins) the UH is synthesized. Commonly used synthetic UHs include the SCS (1972), Snyder (1938), and Clark (1945) methods (see Singh et al., 2014, for a recent review of synthetic UHs). These methods estimate the UH based on relatively few physical characteristics of the watershed. For example, the original SCS/NRCS method used a single dimensionless UH for all watersheds (SCS, 1972). The dimensionless UH was then rescaled based on the coordinates of the UH peak, where the coordinates were typically calculated using watershed characteristics such as the area, mainstream length, and average watershed slope. More recently, the method was updated so that the dimensionless UH shape can vary based on a selected peaking factor (NRCS, 2007).

Watersheds exhibit differences beyond those directly considered in traditional synthetic UH methods. In particular, they can exhibit very distinct channel network structures depending on the geomorphic conditions under which the networks developed. These differences have led to network classifications such as dendritic, parallel, pinnate, rectangular, and trellis (Fig. 1.1) (Howard, 1967; Mejía and Niemann, 2008; Parvis, 1950; Zernitz, 1932). Dendritic networks are tree-like with channels oriented in many directions and acute angles at confluences. This network type develops when few lithologic or topographic constraints are present (Zernitz, 1932). Parallel networks have major channels that are aligned with each other and develop when the region has a pre-existing slope (Castelltort et al., 2009; Howard, 1967; Phillips and Schumm, 1987; Zernitz, 1932). Pinnate networks tend to be feather-like with a single main channel and many smaller channels joining the main channel at acute angles, but the origin of this network type is unclear (Jung et al., 2011; Parvis, 1950; Phillips and Schumm, 1987; Zernitz, 1932). Rectangular networks have channels with right-angle bends and tributaries that merge at right angles. They form when the channels exploit orthogonal jointing in the bedrock (Howard, 1967). Trellis networks resemble a garden trellis with numerous short tributaries joining irregular main streams. This network type develops in fold-and-thrust belts like the Appalachian Mountains (Parvis, 1950; Zernitz, 1932). Channel networks are often classified by visual inspection, but quantitative methods have been developed to ensure objectivity. These methods include empirical approaches (Argialas et al., 1988; Hadipriono et al., 1990; Ichoku and Chorowicz, 1994) and an approach based on scaling invariance (Mejía and Niemann, 2008). The network classification has also been shown to affect the time of concentration of a watershed. For example, Jung et al. (2017) showed differences in relationships between time of concentration with bifurcation ratio and maximum hydraulic length of flow path between network types.

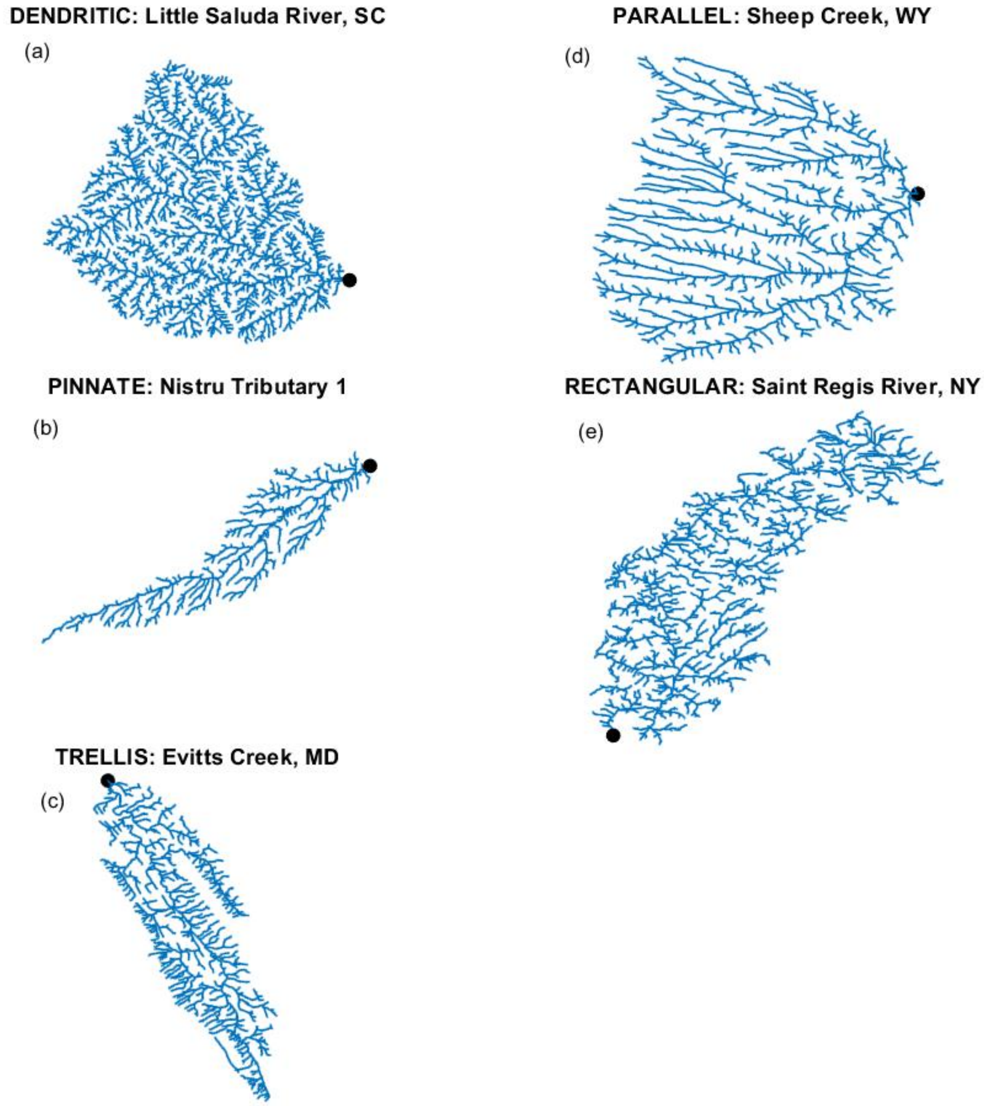

Figure 1.1 A typical channel network from each network classification. Black dots indicate the basin outlets.

Several UH methods have been developed to consider channel network structure, but none have explicitly considered network classifications. The Geomorphologic Instantaneous UH estimates the probability density function (PDF) of travel times using Horton's Ratios, which are derived from the network structure (Gupta et al., 1980; Rodríguez-Iturbe and Valdes, 1979). This approach has also been generalized to allow a nonlinear relationship between excess rainfall and stormflow (Rodríguez-Iturbe et al., 1982) and to consider the effects of hillslope travel times (van der Tak and Bras, 1990). Gupta and Waymire (1983) also proposed a geomorphic instantaneous UH based on stream links instead of Strahler (1957) stream ordering. Other UH methods explicitly represent the watershed's flow paths. For example, the modified Clark method in HEC-HMS allows the user to enter a time-area distribution, which describes the distribution of travel times to the watershed outlet, but that time-area distribution must be determined outside of the modeling framework (Feldman, 2000). It is usually found using a digital elevation model (DEM). Similarly, spatially distributed travel time (SDTT) methods explicitly represent the flow paths in a watershed using a DEM (Du et al., 2009; Lee et al., 2008; Maidment, 1993; Muzik, 1996). Then they calculate a travel time in each DEM grid cell using its physical properties (Du et al., 2009; Zuazo et al., 2014). The UH is then found from the distribution of travel times from the watershed cells to the outlet. Some SDTT methods also overcome the linearity assumption of UH methods because the travel times vary in time (Du et al., 2009; Lee and Yen, 1997). However, SDTT methods operate on the DEM grid and thus cannot be implemented within semi-distributed (or lumped) models.

The objective of this study is to develop and test a nonlinear synthetic UH method that accounts for the network type. The synthetic UH is developed by adapting an SDTT method. It uses kinematic wave theory to derive flood wave travel time expressions for hillslope and channel cells of a DEM. It then estimates the required characteristics for each cell (e.g., channel slope and width) using simplifications and empirical relationships that are applied throughout the watershed. This step allows the properties of each cell to be estimated based on watershed-wide model parameters. It also isolates the effects of the flow path network in two random variables (one for the hillslopes and one for the channels). These two random variables are then represented using theoretical distributions, and the parameters of those distributions are estimated for the five network types. The resulting synthetic UH is nonlinear and can be implemented inside a semi-distributed (or lumped) model if the user provides the model parameters and selects one of the five network types.

The outline of the paper is as follows. Section 2 presents the analytical framework used to determine the synthetic UHs. Section 3 describes the basins used to evaluate the model for each network type. Section 4 evaluates the synthetic UH results by comparing them to the results of an SDTT method (which explicitly represents that actual flow paths for each basin). It also considers whether the network types produce substantial differences in the synthetic UHs. Finally, Section 5 summarizes the key conclusions of the study.

2. MODEL DEVELOPMENT

2.1 Hillslope Travel Time Distribution

The flood wave travel time for a hillslope cell is based on an expression derived by Wong (1995), who applied the kinematic wave approach to a sloping plane where flow enters from upslope and is generated locally by excess rainfall. If this expression is combined with Manning's equation and written for a hillslope cell at location j, it becomes:

$$\tau_{h,j} = \left(\frac{n_{h,j} L_j}{\sqrt{S_j}} \right)^{0.6} E_j^{-0.4} \left[\left(\lambda_{flow,j} + 1 \right)^{0.6} - \left(\lambda_{flow,j} \right)^{0.6} \right] \tag{1}$$

where $\tau_{h,j}$ is the travel time for hillslope cell j, $n_{h,j}$ is Manning's roughness coefficient, L_j is the flow length, S_j is the slope, E_j is the excess rainfall rate, and $\lambda_{flow,j}$ is the ratio of the flow entering from upslope to the flow that is produced within the plane.

Gironás et al. (2009) modified this expression for use in an SDTT method. The excess rainfall is allowed to vary in time but is constrained to be homogeneous in space, so it becomes E_i where i is an index for time. It is assumed that the excess rainfall is produced uniformly across the basin's DEM, so variable source areas are not considered (Dunne and Black, 1970). Because the excess rainfall rate varies in time, the travel time varies in time and becomes $\tau_{h,i,j}$. In reality, $\lambda_{flow,j}$ also varies in time, but Gironás et al. (2009) made the approximation that $\lambda_{flow,j} = A_{up,j} / A$, where $A_{up,j}$ is the total area that is upslope of the grid cell and A is the area of the grid cell itself. This approach assumes that the duration of the storm is long enough for the entire upslope area to contribute flow simultaneously to the grid cell. This assumption has been made by others (e.g., Melesse and Graham, 2004; Rodríguez-Iturbe et al., 1982) and was evaluated in detail by Zuazo et al. (2014), who found it to be a good approximation of full kinematic wave routing on hillslopes. Using these approximations, Eq. (1) becomes:

$$\tau_{h,i,j} = \left(\frac{n_{h,j} L_j}{\sqrt{S_j}} \right)^{0.6} E_i^{-0.4} \left[\left(\frac{A_{up,j}}{A} + 1 \right)^{0.6} - \left(\frac{A_{up,j}}{A} \right)^{0.6} \right] \tag{2}$$

Even though every grid cell has the same area A, the length L_j can vary between grid cells to account for flow paths in the diagonal and cardinal directions of the grid.

An expression can then be written for the total hillslope travel time ($T_{h,i,k}$) for flow that starts at any cell k in the basin and moves to the basin outlet:

$$T_{h,i,k} = \sum_{j \in \text{Hillslope}} \left(\frac{n_{h,j} L_j}{\sqrt{S_j}} \right)^{0.6} E_i^{-0.4} \left[\left(\frac{A_{up,j}}{A} + 1 \right)^{0.6} - \left(\frac{A_{up,j}}{A} \right)^{0.6} \right] \tag{3}$$

where the summation includes all the hillslope cells on the path between cell k and the basin outlet. Eq. (3) indicates that the hillslope travel time depends on a variety of local characteristics. To simplify the model, three approximations are implemented. First, variation in the local flow length is neglected by replacing L_j with L, which is an effective flow length for all grid cells. Assuming that flow directions are equally likely to occur in all cardinal and diagonal directions, that effective length is the average of the cardinal and diagonal flow lengths of the grid cells ($L = 0.5\left(1+\sqrt{2}\right)A^{0.5}$). Second, all hillslope cells are assumed to have the same roughness n_h, which is frequently assumed when applying similar models (e.g., Gironás et al., 2009; Robinson and Sivapalan, 1996; Zuazo et al., 2014). Third, it is assumed that all hillslope cells have the same effective slope S_h. In reality, most basins tend to have convex-up hillslopes due to slope-dependent transport processes, such as rain splash, bioturbation, and soil creep (Gilbert, 1909; Roering et al., 2001; Tucker and Bras, 1998). However, planar hillslopes are a common assumption in many similar models (e.g., Gironás et al., 2009; Robinson and Sivapalan, 1996). Using these approximations, the total hillslope travel time becomes:

$$T_{h,i,k} = E_i^{-0.4} n_h^{0.6} S_h^{-0.3} L^{-0.4} \sum_{j \in \text{Hillslope}} L\left[\left(\frac{A_{up,j}}{A}+1\right)^{0.6} - \left(\frac{A_{up,j}}{A}\right)^{0.6}\right] \tag{4}$$

To simplify the notation, the constant basin properties are collected into a single hillslope coefficient $m_h \equiv n_h^{0.6} S_h^{-0.3} L^{-0.4}$. In addition, the summation in Eq. (4) is defined as $A_{sh,k}$, where the subscript k is included because each location where flow starts k has a different path to the outlet and thus a different value for that summation. This summation depends on the accumulation of area along the hillslope flow paths, so it is closely related to the aggregation of the flow network. Substituting these variables into Eq. (4), it becomes:

$$T_{h,i,k} = E_i^{-0.4} m_h A_{sh,k} \tag{5}$$

Eq. (5) describes the hillslope travel time from an arbitrary point k to the outlet. For a given storm event, flow is expected to begin at all locations in the basin. Thus, one can consider $A_{sh,k}$ as the outcome (for location k) of a random variable A_{sh}. The variable A_{sh} probabilistically describes the collection of values of $A_{sh,k}$ that occur across the basin. It is assumed that A_{sh} is described by the Johnson Special Bounded (SB) distribution (this assumption is evaluated later). This distribution is related to the normal distribution, which is associated with sums (George and Ramachandran, 2011; Kottegoda, 1987), and $A_{sh,k}$ is a sum, as shown in Eq. (4). The Johnson SB PDF is written:

$$f(A_{sh}) = \frac{\delta_h \lambda_h}{\sqrt{2\pi}\left(A_{sh}-\xi_h\right)\left(\lambda_h - A_{sh} + \xi_h\right)} \exp\left\{-\frac{1}{2}\left[\gamma_h + \delta_h \ln\left(\frac{A_{sh}-\xi_h}{\lambda_h - A_{sh}+\xi_h}\right)\right]^2\right\} \tag{1}$$

where γ_h is a shape parameter that primarily controls the skewness, and δ_h is a second shape parameter that primarily controls the kurtosis. ξ_h is the location parameter, and λ_h is the scale parameter. It is assumed that γ_h, δ_h, ξ_h, and λ_h can be estimated from the network type and maximum upslope area for any hillslope cell A_{hmax}. These assumptions and the nature of any such dependence is examined later.

2.2 Channel Travel Time Distribution

A very similar approach is used to calculate the travel time distribution for the channels. The flood wave travel time in a channel cell is based on an expression derived by Wong (2001), who considered a wide rectangular channel where flow enters from both upstream and locally under the kinematic wave approximation. If the Wong (2001) equation is applied to a channel cell at location j, it can be written:

$$\tau_{c,j} = L_j \left(\frac{n_{c,j}}{\sqrt{S_j}} \right)^{0.6} W_j^{0.4} \left[\frac{Q_{down,j}^{0.6} - Q_{up,j}^{0.6}}{Q_{down,j} - Q_{up,j}} \right] \tag{7}$$

where $\tau_{c,j}$ is the travel time in channel cell j, $n_{c,j}$ is Manning's roughness coefficient for the cell, W_j is the channel width, $Q_{down,j}$ is the flow at the downstream end of the cell, and $Q_{up,j}$ is the flow that is contributed to the cell from upstream. Unlike the hillslope cells, which drain relatively small areas, it is unlikely that the entire upstream area simultaneously contributes flow to a channel cell for storms with realistic durations. Following Iacobellis and Fiorentino (2000), it is assumed that only some fraction r of the upstream area contributes flow simultaneously. Thus, $Q_{up,j} = rE_i A_{up,j}$ and $Q_{down,j} = rE_i \left(A_{up,j} + A \right)$ if excess rainfall is again assumed to be spatially homogeneous.

An expression can then be written for the total channel travel time from a cell k in the basin to the basin outlet $T_{c,i,k}$:

$$T_{c,i,k} = \sum_{j \in \text{Channel}} L_j \left(\frac{n_{c,j}}{\sqrt{S_j}} \right)^{0.6} \left(\frac{W_j}{rE_i} \right)^{0.4} \left[\frac{\left(A_{up,j} + A \right)^{0.6} - A_{up,j}^{0.6}}{A} \right] \tag{8}$$

where the summation includes the channel cells on the path between cell k and the outlet.

Several approximations are implemented to simplify Eq. (8). Local variations in cell flow lengths are again neglected by replacing L_j with L, and all channel cells are assumed to have the same roughness n_c, which is a common approach (e.g., Gironás et al., 2009; Zuazo et al., 2014). In addition, the channel slope is assumed to depend on the contributing area according to a power function $S_j = b(A_{up,j} + A)^{-\theta}$ where b and θ are constants that can vary between basins (Flint, 1974; Hack, 1957; Sklar and Dietrich, 2013; Tarboton et al., 1989; Willgoose et al., 1991). The coefficient b is related to the vertical relief of the basin, while θ describes the concavity of the longitudinal profiles of the channels. The slope-area relationship describes the average slope at a given contributing area, but much variation typically occurs around this average value (Cohen et al., 2008; Niemann et al., 2001; Tarboton et al., 1989). In addition, deviations from a power function can also occur (Ijjasz-Vasquez and Bras, 1995). Such complexities are neglected here. Finally, the channel width is also assumed to depend on the contributing area according to a power function $W_j = d(A_{up,j} + A)^e$ where d and e are constants that can vary between basins. Such dependence has been observed empirically (Hack, 1957; Leopold and Maddock, 1953; Montgomery and Gran, 2001; Wolman, 1955) and has been used in similar models in the past (Snyder et al., 2003). Employing these simplifications in Eq. (8), one obtains:

$$T_{c,i,k} = E_i^{-0.4} n_c^{0.6} r^{-0.4} b^{-0.3} d^{0.4} A^{0.3\theta+0.4e-0.4} \sum_{j \in \text{Channel}} L \left(\frac{A_{up,j}}{A} + 1 \right)^{0.3\theta+0.4e} \left[\left(\frac{A_{up,j}}{A} + 1 \right)^{0.6} - \left(\frac{A_{up,j}}{A} \right)^{0.6} \right] \tag{9}$$

To simplify the notation, the constants in front of the summation are collected into a single channel coefficient $m_c \equiv r^{-0.4} n_c^{0.6} b^{-0.3} d^{0.4} A^{0.3\theta+0.4e-0.4}$, and the summation in Eq. (9) is defined as $A_{sc,k}$. This variable describes how area accumulates along the channel flow path and is expected to depend on the channel network structure. Using these definitions, Eq. (9) can be written:

$$T_{c,i,k} = E_i^{-0.4} m_c A_{sc,k} \tag{10}$$

It is assumed that A_{sc} is described by the Johnson special bounded (SB) distribution:

$$f(A_{sc}) = \frac{\delta_c \lambda_c}{\sqrt{2\pi}\left(A_{sc} - \xi_c\right)\left(\lambda_c - A_{sc} + \xi_c\right)} \exp\left\{-\frac{1}{2}\left[\gamma_c + \delta_c \ln\left(\frac{A_{sc} - \xi_c}{\lambda_c - A_{sc} + \xi_c}\right)\right]^2\right\} \tag{11}$$

Where γ_c primarily controls the skewness, and δ_c primarily controls the kurtosis. ξ_c is the location parameter, and λ_c is the scale parameter. It is assumed that γ_c, δ_c, ξ_c, and λ_c and can be estimated based on the network type and maximum upstream area for any channel cell $A_{\max}$. The nature of any such dependence is examined later.

2.3 Total Travel Time Distribution

The total travel time from an arbitrary point k to the outlet ($T_{i,k}$) is the sum of the hillslope and channel travel times from that point, so one can write:

$$T_{i,k} = T_{h,i,k} + T_{c,i,k} = E_i^{-0.4}\left(m_h A_{sh,k} + m_c A_{sc,k}\right) \tag{12}$$

If the time-invariant portion of the overall travel time is defined as $X_k \equiv m_h A_{sh,k} + m_c A_{sc,k}$, then the PDF for X can be determined by a convolution assuming that $m_h A_{sh,k}$ and $m_c A_{sc,k}$ are independent. The hillslope scale is typically similar irrespective of the hillslope's position in the basin (Tucker et al., 2001), so the hillslope and channel travel times from a point to the outlet are expected to be independent (Rodríguez-Iturbe and Valdes, 1979). Because an analytical solution for this convolution is not known, the convolution is performed numerically:

$$f_X\left(n\Delta X\right) = \sum_{l=0}^{n} f_{m_h A_{sh,k}}\left(l\Delta X\right) f_{m_c A_{sc,k}}\left(n\Delta X - l\Delta X\right) \tag{13}$$

where n is the number of discrete increments of X used in the numerical evaluation, ΔX is the size of the increment, and l is an index for those increments. Finally, the instantaneous UH (IUH) associated with excess rainfall E_i can be found from the PDF for T_i, which is:

$$f_{T_i}\left(T_i\right) = \frac{1}{E_i^{-0.4}} f_X\left(\frac{T_i}{E_i^{-0.4}}\right) \tag{14}$$

The IUH varies in time because E_i varies in time. UHs and direct runoff hydrographs can then be calculated by a convolution of the excess rainfalls and IUHs as described by Gironás et al. (2009).

In summary, this modeling approach isolates the effect of the drainage network structure in the random variables A_{sh} and A_{sc}. The other basin properties are represented by a series of constants (n_h, S_h, n_c, r, b, d, θ, and e), which can be set for the basin of interest. The method also includes two constants that imply the spatial resolution of the calculations: L and A. These constants transform the PDFs for A_{sh} and A_{sc} into the time-invariant PDF for X. Then the PDF for X is modified using the time-varying excess rainfall rate E_i to determine the time-varying PDF for T_i, which is the time-varying IUH for the basin.

This method is similar to the time-area methods developed by Zoch (1934) and Clark (1945) because it uses travel times that are determined from the basin shape. Those methods used simplified watershed geometries, but that approach has since been generalized to use real watershed configurations (Kull and Feldman, 1998; Peters and Easton, 1996; Saghafian et al., 2002). The proposed model also differs from those methods because the travel times vary in time, which produces a time-varying IUH. The use of time-varying UHs has also been explored by others (Du et al., 2009; Lee et al., 2008; Xia et al., 2005). Also, those methods used a linear reservoir to represent the attenuation of the flood wave by storage in the basin (Clark, 1945; Zoch, 1934). The effects of including a linear reservoir in the proposed synthetic UH method will be explored later in this paper.

3. APPLICATION TO BASINS

The synthetic UH method is evaluated by application to 10 basins from each of the five classifications. Nearly all the basins were originally processed by Mejía and Niemann (2008). In their collection, however, Buckeye Run, WV, (dendritic) and Stony Run, WV, (trellis) are sub-basins of other included basins. Furthermore, Hill Creek, UT, (parallel) does not strongly exhibit parallel characteristics. Thus, these three basins were replaced with Rockcastle Creek, KY, (dendritic), Penns Creek, PA, (trellis), and Mancos River Tributary, CO, (parallel). The new basins were selected from regions where the networks had been previously classified (Mejía and Niemann, 2008).

The new basins were processed in the manner used by Mejía and Niemann (2008). Specifically, the TauDEM toolbox for ArcGIS was used to fill pits, determine flow directions (according to the D8 algorithm), and calculate upslope/upstream areas and slopes (O'Callaghan and Mark, 1984; Tarboton, 2003; Tarboton et al., 1991). To avoid infinite travel times in the model, any zero slope was replaced by the lesser of the calculated slope resolution and 0.8 times the minimum nonzero slope present in the processed DEM.

A cell is considered to contain a channel if the contributing area exceeds a selected threshold. Montgomery (2001) divided the slope-area plot into five geomorphic zones (hillslopes, valley heads, colluvial channels, bedrock channels, and alluvial channels), and we evaluated two threshold areas based on these zones. The first threshold separates the valley heads and colluvial channels, and the second distinguishes the colluvial and bedrock channels. The presented results use the second threshold because it avoids producing unrealistic adjacent, parallel channels at small contributing areas (the results when the first threshold is used are discussed later).

Basic characteristics for the 50 basins are summarized in Table 3.1. The pinnate basins tend to be larger than the other types with an average area of 1,014 km^2. The parallel and rectangular basins are the smallest with average areas of 217 and 254 km^2, respectively. The pinnate basins also have the coarsest DEM resolutions with an average of 76.4 m, while the DEM resolutions for the remaining types are, on average, 27 m. The channel threshold area (which also determines $A_{h\max}$) is largest for pinnate basins (on average 688,560 m^2) and smallest for dendritic and parallel basins (on average 53,720 and 76,850 m^2, respectively).

Table 3.1 Basic characteristics of the 50 basins analyzed in this study

	Basin Name	Outlet Lat. (deg)	Outlet Long. (deg)	DEM Resolution (m)	Basin Area (km^2)	Channel Threshold (m^2)
DENDRITIC	Bluestone Creek, WV	39.3020	-80.7787	27.2	324	33,300
	Buffalo Creek, WV	40.2509	-80.5976	27.0	419	56,000
	Captina Creek, OH	39.8706	-80.8193	27.0	460	29,200
	Cedar Creek, GA	31.6712	-81.5048	28.5	219	115,500
	Little Saluda River, SC	34.0773	-81.5942	28.1	565	102,900
	Rockcastle Creek, KY	38.0020	-82.5189	27.9	314	53,400
	Tenmile Creek, PA	39.9804	-80.0240	27.0	512	95,500
	Turkey Creek, SC	33.7773	-82.1606	30.0	625	63,000
	Tygarts Creek, KY	38.3926	-82.9601	27.4	291	79,100
	Wheeling Creek, WV	40.0506	-80.6673	27.0	739	36,500
PARALLEL	Albert Creek, WY	41.5065	-110.6095	26.8	439	57,400
	Black Sulphur Creek, CO	39.8676	-108.2931	27.1	266	73,300
	Duck Creek, CO	39.9787	-108.3820	27.0	142	80,300
	Greasewood Creek, CO	40.1301	-108.4126	27.0	61	65,200
	Mancos River Trib., CO	37.0950	-108.5070	28.3	113	133,100
	Piceance Tributary 1, CO	39.8884	-108.3959	27.1	156	70,600
	Piceance Tributary 2, CO	39.8620	-108.2998	27.1	74	47,600
	Sheep Creek, WY	41.5645	-110.6154	26.8	487	215,100
	Willow Creek, UT	39.4223	-109.6293	27.2	350	55,400
	Yellow Creek, CO	39.9654	-108.3898	27.1	85	110,000
PINNATE	Dniester Tributary 1, UKR	47.9145	30.6362	75.9	2,114	1,037,900
	Dniester Tributary 2, UKR	48.1245	30.0062	75.8	1,356	488,500
	Dniester Tributary 3, UKR	46.3545	28.9412	76.8	1,005	707,800
	Dniester Tributary 4, UKR	46.7937	29.9804	76.4	1,573	540,300
	Dniester Tributary 5, UKR	46.6145	29.2845	76.7	967	706,700
	Dniester Tributary 6, UKR	47.1395	28.9062	76.4	761	1,045,100
	Nistru Tributary 1, MDA	47.3795	30.5062	76.2	697	639,400
	Nistru Tributary 2, MDA	47.3895	30.5562	76.4	589	758,400
	Nistru Tributary 4, MDA	46.1112	28.6129	76.8	723	614,600
	Nistru Tributary 5, MDA	46.0529	28.7587	76.8	350	983,800
RECTANGULAR	Boquet River, NY	44.2423	-73.4620	26.2	241	108,500
	Boreas River, NY	43.8320	-74.0709	26.3	218	250,500
	Cold River NY	44.1037	-74.3126	26.2	218	104,300
	Hudson River, NY	43.9681	-74.0526	26.3	198	239,700
	Saint Regis River, NY	44.5320	-74.4723	26.1	344	124,600
	Salmon River, NY	44.8673	-74.2970	26.1	495	146,200
	Schroon River, NY	43.9556	-73.7337	26.3	239	172,300
	Summer Brook, NY	44.4076	-74.0837	26.1	147	88,900
	Walker Brook, NY	44.0004	-73.7126	26.2	133	198,400
	W. Br. St. Regis River, NY	44.4387	-74.5912	26.1	304	116,100
TRELLIS	Aughwick Creek, PA	40.2987	-77.8873	27.0	823	141,700
	Cacapon River, WV	39.2533	-78.4549	28.0	865	125,100
	Chestuee Creek, TN	35.2451	-84.6565	27.9	339	54,300
	Evitts Creek, MD	39.6640	-78.7320	27.1	240	168,600
	Jackson River, VA	39.1651	-79.7509	27.4	251	116,300
	Juniata River, PA	40.5070	-77.4381	27.5	539	62,700
	Middle Creek, PA	40.7643	-76.8845	26.8	219	166,300
	Penns Creek, PA	40.85756	-77.4606	27.5	480	956,900
	Peters Run, WV	38.7229	-79.3043	27.3	609	59,600
	Sleepy Creek, WV	39.6206	-78.1459	27.1	294	51,500

4. RESULTS

4.1 Evaluation of Model Assumptions

We first examine the distributions of A_{sh} and A_{sc} for the basins. In order to calculate A_{sc} for any basin, values must be selected for the width-area exponent e and the slope-area exponent θ. e was assigned a typical value of 0.5 for all basins based on Montgomery and Gran (2001). θ was calculated from the slope-area plot of each basin. It has averages of 0.37, 0.43, 0.35, 0.38, and 0.39, for the dendritic, parallel, pinnate, rectangular, and trellis basins, respectively. Because θ might vary with the network type, A_{sc} for a given basin was calculated using that basin's θ value.

Twenty-four theoretical distributions were identified as candidates to describe A_{sh} and A_{sc} based on their general properties (e.g., the existence of a lower bound). The parameters of the distributions were estimated for each basin using the Easyfit software, which uses different estimation methods depending on the type of distribution (maximum likelihood, L-moments, etc.). The fit of each distribution was then evaluated using the Kolmogorov-Smirnov (K-S) statistic, which is the maximum deviation between the cumulative distribution function (CDF) determined from the DEMs and the theoretical distribution (D'Agostino and Stephens, 1986; Weber et al., 2006). The K-S statistic is not compared to a critical value in a hypothesis test because the observations of A_{sh} and A_{sc} from the DEMs are not independent due to the nested structure of the drainage networks. Thus, they violate the assumptions required to perform such a test (D'Agostino and Stephens, 1986; Jogesh Babu and Rao, 2004).

The K-S statistics for the four best-fitting distributions for A_{sh} and A_{sc} are plotted for all basins in Figure 4.1. The four best distributions for A_{sh} are the generalized extreme value, three-parameter Weibull, four-parameter generalized gamma, and Johnson SB (Fig. 4.1a). The Johnson SB distribution fits the observations of A_{sh} best with an average K-S statistic of 0.014. Among the considered distributions, it also produces the lowest average K-S statistic for each classification except rectangular. Overall, these results suggest that the Johnson SB distribution is the best choice for representing A_{sh}. The four best distributions for A_{sc} are the generalized extreme value, PERT, four-parameter generalized gamma, and Johnson SB (Fig. 4.1b). On average, the Johnson SB distribution fits the observed CDFs of A_{sc} best with an average K-S statistic of 0.023. The Johnson SB distribution also exhibits the best average K-S statistic for each classification. Overall, the results suggest that the Johnson SB distribution is also the best choice for representing A_{sc}.

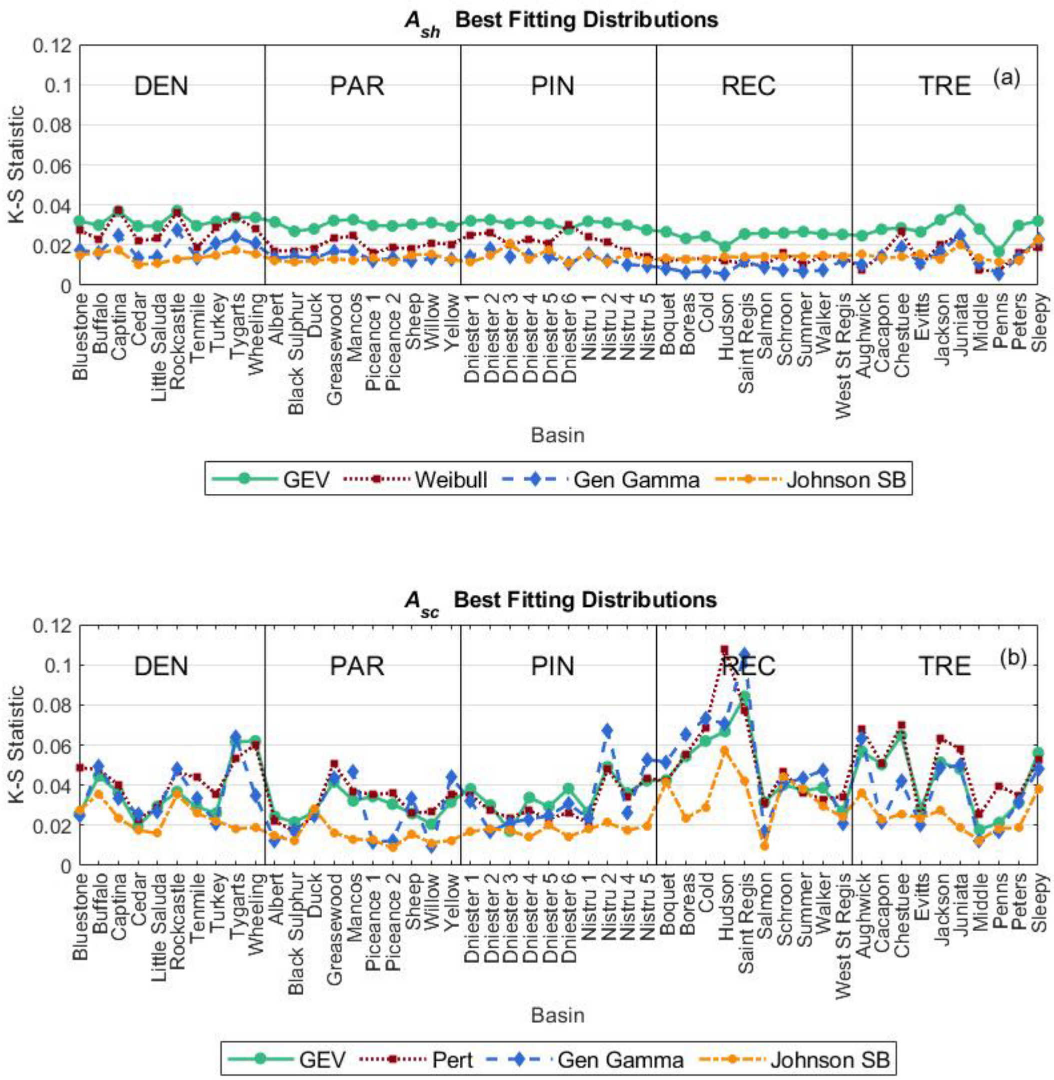

Figure 4.1 Kolmogorov-Smirnov (K-S) statistics for the four best fitting distributions for (a) A_{sh} and (b) A_{sc}. DEN denotes dendritic, PAR denotes parallel, PIN denotes pinnate, REC denotes rectangular, and TRE denotes trellis.

Figure 4.2 (left side) shows the histogram of A_{sh} values for a typical basin in each classification along with the fitted PDF. The A_{sh} distributions always have positive skewness, but the degree of peakedness and skewness varies between the classifications. Specifically, the rectangular and trellis basins have more apparent peaks and skewness than the other classifications. In all cases, the Johnson SB distribution fits the histograms well. The A_{sc} distributions differ substantially among the five basins (Fig. 4.2, right side). Notably, the A_{sc} distribution has negative skewness for the dendritic and parallel basins. It is nearly symmetrical for the trellis basin and has positive skewness for the pinnate and rectangular basins. The Johnson SB distribution fits histograms well, but it misses local fluctuations in some of the histograms.

We next examine whether the parameters of the Johnson SB distribution for A_{sh} can be estimated from the network classification and the hillslope size $A_{h\max}$. For each classification, Figure 4.3 plots the calibrated distribution parameters against $A_{h\max}$. The shape parameters δ_h and γ_h and the location parameter ξ_h appear to be independent of $A_{h\max}$ and relatively constant within each classification. However, differences are observed in the parameter values for different classifications. The rectangular and trellis basins tend to have higher δ_h and γ_h values than the other basin types. Higher δ_h values produce more peaked distributions, and higher γ_h values produce greater skewness. Thus, these results confirm that the differences observed for the example basins are typical for the classifications. The scale parameter λ_h depends on $A_{h\max}$ (Fig. 4.3d), and this dependence appears to differ between classifications. The relationships can be approximated by power functions (a power function is preferable to a line because it always passes through the origin as expected for both A_{sh} and A_{sc}). Most notably, the pinnate and trellis basins have steeper power functions than the other types.

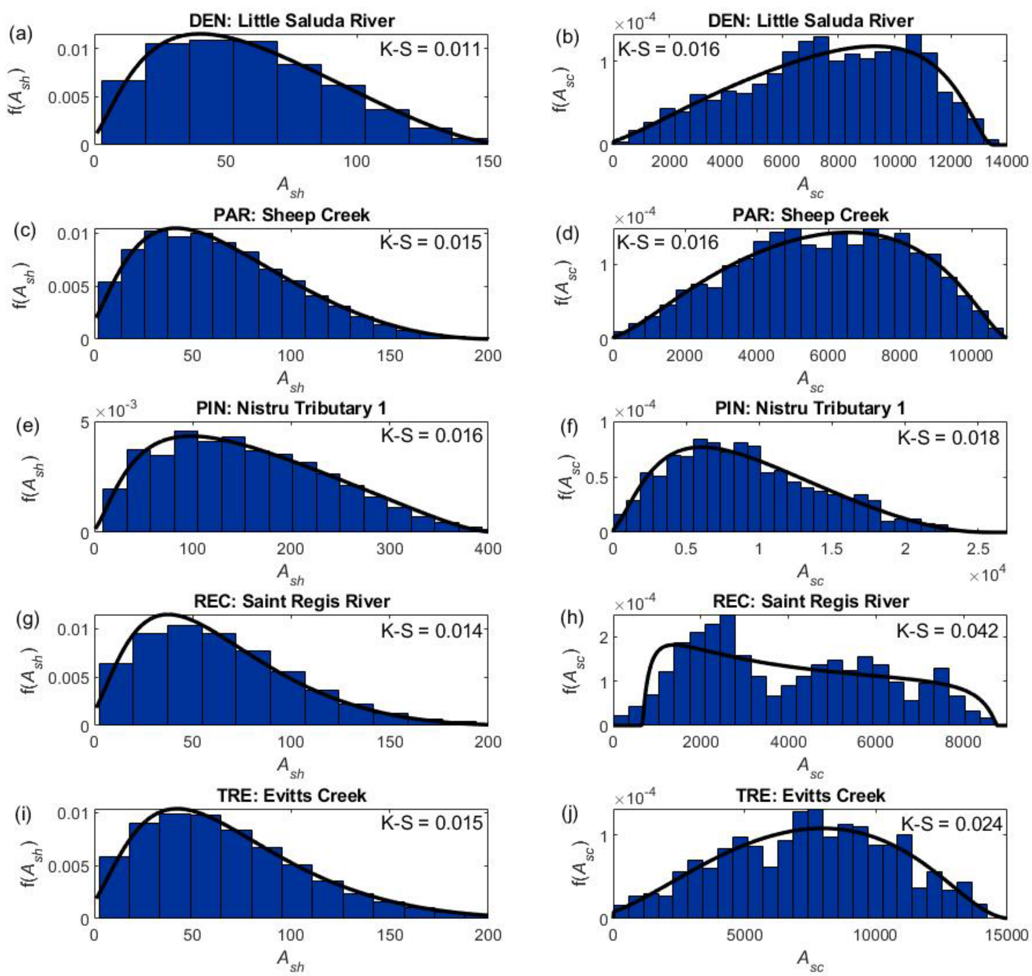

Figure 4.2 Histograms and fitted Johnson SB distributions for A_{sh} (left column) and A_{sc} (right column) for a typical basin in each classification. The basins are the same as those in Figure 1.1

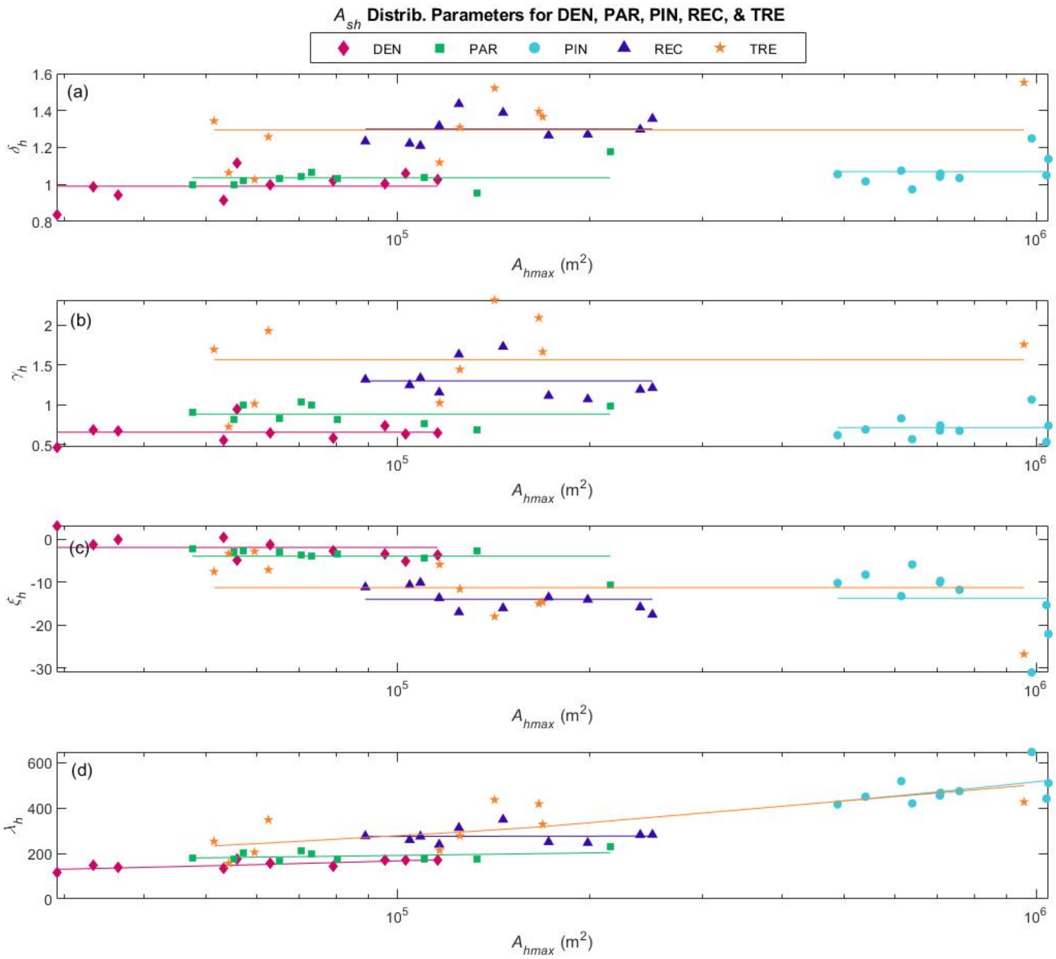

Figure 2.3 Parameters of the Johnson SB distribution for A_{sh} plotted against the maximum hillslope area $A_{h\max}$. The symbols show the calibrated parameter values for each basin. The horizontal lines in (a) – (c) show the average parameter value for each network type. The lines in (d) show power functions fitted to the λ_h values for each network type.

We next consider whether the parameters of the Johnson SB distribution for A_{sc} can be estimated from the network type and the basin size $A_{\max}$. For each classification, Figure 4.4 plots the calibrated distribution parameters against $A_{\max}$. The shape parameters δ_c and γ_c and the location parameter ξ_c appear to be independent of $A_{\max}$. δ_c does not appear to differ between the classifications, but the skewness-related parameter γ_c appears to differ. Dendritic and parallel basins have negative γ_c values, while pinnate basins have positive γ_c values (which is consistent with the example basins in Figure 4.2). The skewness also relates to the typical basin shape for each classification seen in Figure 1.1. For example, dendritic and parallel basins have an abundance of channel cells far from the basin outlet, which leads to an abundance of large A_{sc} values and negative skewness. In contrast, the pinnate basin has fewer points at the greatest distance from the outlet, which leads to a positive skewness. The scale parameter λ_c varies with $A_{\max}$, and the observed relationships can be approximated with power functions. The power functions may differ between certain classifications. Specifically, the power function for pinnate basins is much higher in the graph than the power function for rectangular basins.

Table 4.1a provides the average values of δ_h, γ_h, and ξ_h for each classification (and average values for all basins combined). It also provides the fitted power function that estimates λ_h from $A_{h\max}$ for each classification (and a fitted power function for all basins combined). Table 4.1b provides equivalent information for γ_c, δ_c, ξ_c, and λ_c. To determine whether the distribution parameters differ significantly between the network types, an analysis of variance (ANOVA) was employed for the parameters that are independent of $A_{h\max}$ and $A_{\max}$. Specifically, a one-way ANOVA was used for unadjusted pairwise comparisons between classifications (Cohen and Cohen, 2008) with a 90% confidence interval (p-value = 0.1). Similarly, an analysis of covariance (ANCOVA) was used to determine whether the coefficients and exponents of the power functions are significantly different between classifications (Maxwell and Delaney, 2004). This analysis was performed by first taking the logarithms of the variables involved and examining whether the intercepts and slopes of the resulting linear relationships are different.

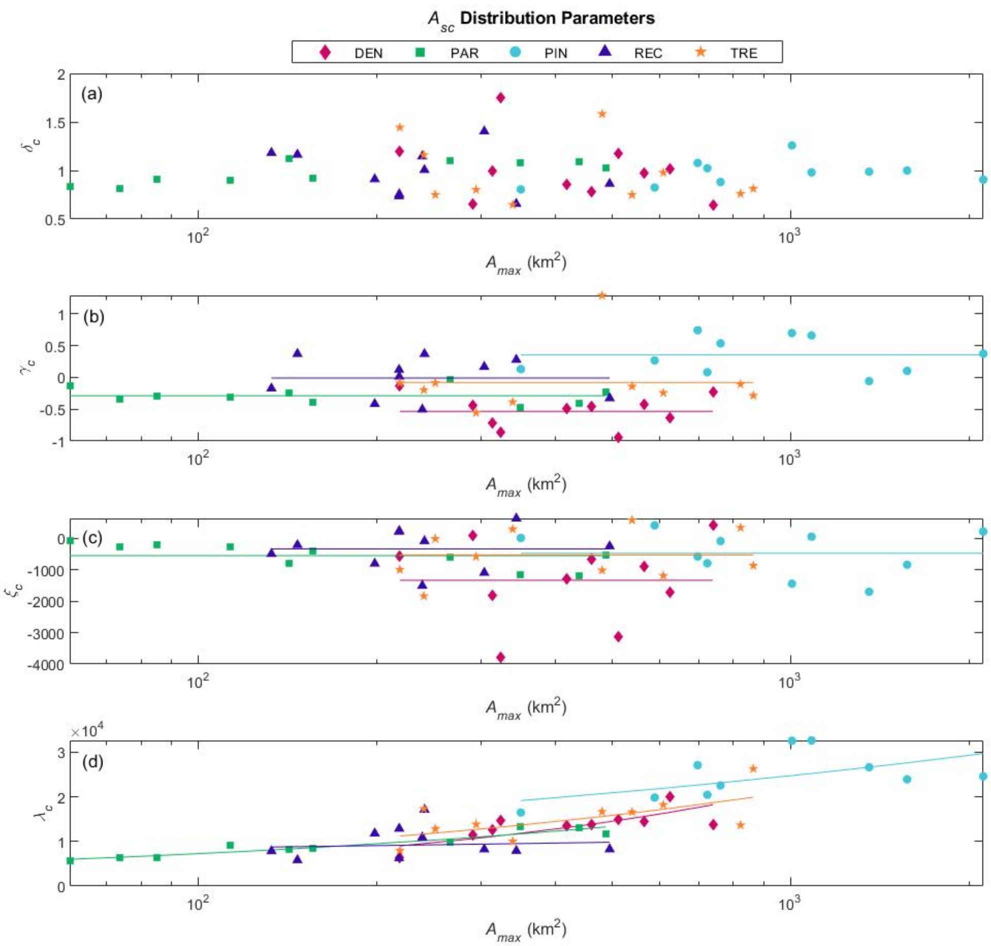

Figure 4.4 Parameters of the Johnson SB distribution for A_{sc} plotted against the maximum upstream area $A_{\max}$. The symbols show the calibrated parameter values for each basin. The horizontal lines in (b) – (c) show the average parameter value for each network type. The lines in (d) show power functions fitted to the λ_c values for each network type.

Table 4.1 Estimated parameters for the Johnson SB distributions for (a) A_{sh} and (b) A_{sc}

(a) A_{sh}

	δ_h	γ_h	ξ_h	λ_h
Dendritic	0.991	0.654	-1.8	$16\,A_{h\max}^{0.204}$
Parallel	1.036	0.881	-3.9	$76\,A_{h\max}^{0.081}$
Pinnate	1.069	0.711	-13.7	$15\,A_{h\max}^{0.255}$
Rectangular	1.300	1.300	-14.0	$258\,A_{h\max}^{0.006}$
Trellis	1.296	1.567	-11.2	$14\,A_{h\max}^{0.256}$
All	1.138	1.023	-8.9	$3\,A_{h\max}^{0.373}$

(b) A_{sc}

	δ_c	γ_c	ξ_c	λ_c
Dendritic	-	-0.533	-1339	$398\,A_{\max}^{0.579}$
Parallel	-	-0.288	-556	$1256\,A_{\max}^{0.381}$
Pinnate	-	0.352	-479	$4579\,A_{\max}^{0.244}$
Rectangular	-	-0.011	-341	$5687\,A_{\max}^{0.088}$
Trellis	-	-0.081	-533	$1203\,A_{\max}^{0.414}$
All	0.982	-0.112	-649	$668\,A_{\max}^{0.504}$

The results of the ANOVA and ANCOVA tests are summarized in Table 4.2. If a parameter is listed in Table 4.2, there is a 90% chance that the pair of classifications have different mean values for that parameter. For A_{sh} , all 10 classification pairs have at least one parameter that is significantly different (Table 4.2a). Thus, the differences identified visually in Figures 4.2 and 4.3 are consistent enough between classifications to be significant. For A_{sc} , eight out of 10 classification pairs have at least one parameter that is significantly different (Table 4.2b). Most commonly, the different parameter is γ_c , which is associated with skewness. In contrast, δ_c never differs between classifications. Fewer parameters are significantly different for A_{sc} than A_{sh} because the parameters for A_{sc} tend to be more variable within classifications. Overall, these results confirm that the distributions for A_{sh} and A_{sc} are different between the five network classifications.

Table 4.2 Distribution parameters that exhibit significant differences between the network types based on the analysis of variance (ANOVA) and analysis of covariance (ANCOVA) tests. For each classification paring, the top row reports parameters for A_{sh} , and the bottom row reports parameters for A_{sc} . For the scale parameters, "coef" indicates the power function coefficient and "exp" indicates the exponent.

(a) A_{sh}

	DEN	PAR	PIN	REC	TRE
DEN		γ_h	δ_h , ξ_h , $\lambda_h$coef , $\lambda_h$exp	δ_h , γ_h , ξ_h	δ_h , γ_h , ξ_h
PAR			ξ_h	δ_h , γ_h , ξ_h	δ_h , γ_h , ξ_h , $\lambda_h$coef , $\lambda_h$exp
PIN				δ_h , γ_h	δ_h , γ_h , ξ_h , $\lambda_h$coef , $\lambda_h$exp
REC					ξ_h , $\lambda_h$coef , $\lambda_h$exp

(b) A_{sc}

	DEN	PAR	PIN	REC	TRE
DEN		ξ_c	γ_c , ξ_c , $\lambda_c$coef	γ_c , ξ_c , $\lambda_c$coef	γ_c , ξ_c
PAR			γ_c	γ_c	–
PIN				γ_c	γ_c
REC					–

To evaluate the reliability of estimating the distribution parameters from the network type (as well as $A_{h\max}$ and $A_{\max}$), the K-S statistic is used once more. Figure 4.5 compares the K-S statistics for the basins when the distribution parameters are estimated from three different methods. In Method 1, they are calibrated directly from the A_{sh} and A_{sc} distributions for each basin (i.e. using the individual values shown in Figs. 4.3 and 4.4). In Method 2, they are estimated from the classification (using the results for each classification in Table 4.1). In Method 3, they are estimated without consideration of the classification (using the results for all basins combined in Table 4.1).

Comparing Methods 3 and 2 for A_{sh}, 44 of the 50 basins have improved accuracy (lower K-S statistics) when the network type is included (Fig. 4.5a). The average K-S statistic across all basins is 0.095 for Method 3 and 0.037 for Method 2. The improvement occurs for all classifications but is smallest for trellis networks. Thus, considering the network type provides much better estimates of the A_{sh} distribution than neglecting the network type. Comparing Methods 2 and 1 for A_{sh}, the K-S statistics are relatively similar (the average K-S statistic is 0.014 for Method 1). However, Method 1 provides much better K-S statistics for trellis basins (Fig. 4.5a). Thus, the network type provides adequate information for estimating the A_{sh} distribution for most classifications, but explicit consideration of the individual basins is needed for the trellis classification.

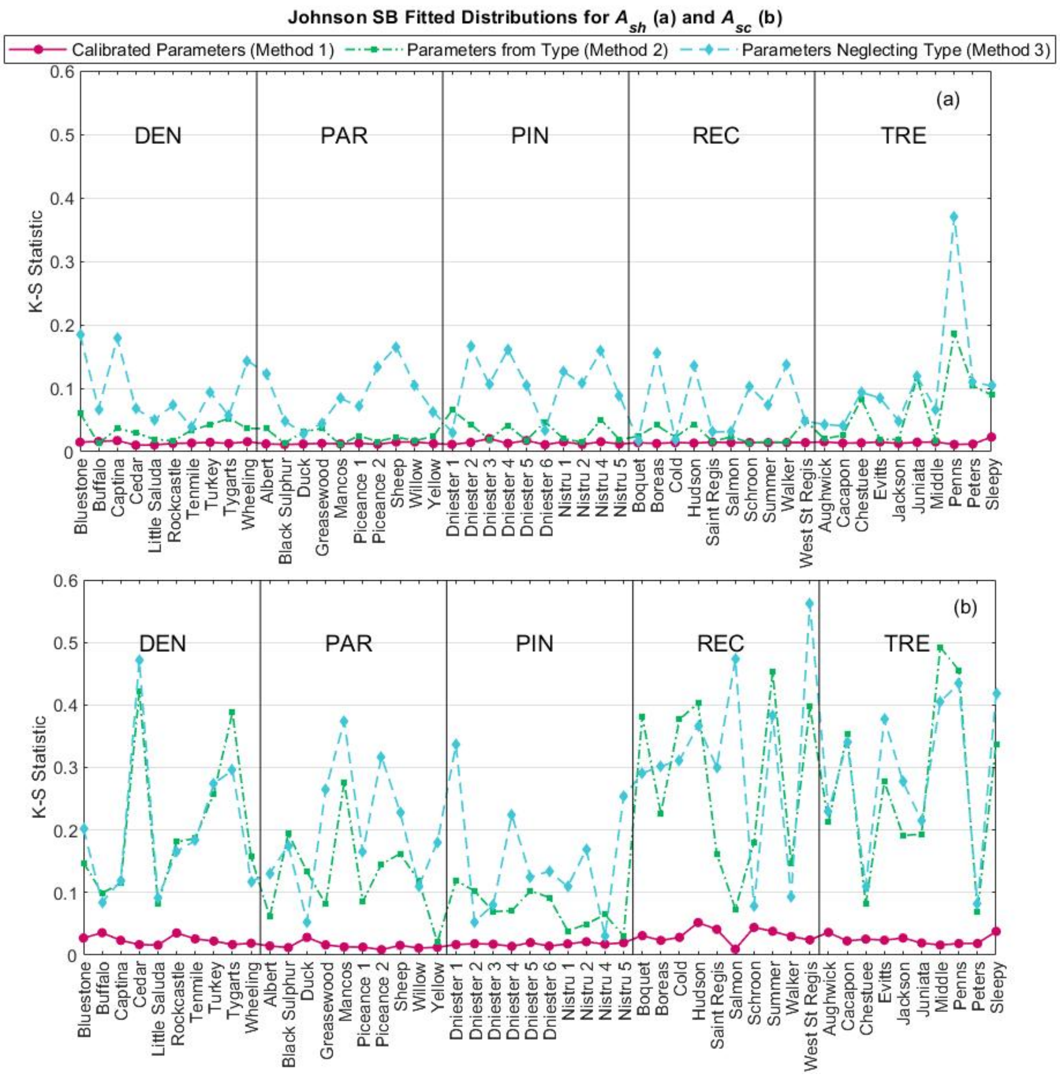

Figure 4.5 Kolmogorov- Smirnov (K-S) statistics for the Johnson SB distribution for (a) A_{sh} and (b) A_{sc} when the distribution parameters are estimated separately for each network (Method 1), based on network classification (Method 2), and neglecting network classification (Method 3).

For A_{sc}, 31 of the 50 basins have improved accuracy (lower K-S statistics) when the network type is included (comparing Methods 3 and 2), but the overall improvement is small (Fig. 4.5b). The average K-S statistic is 0.231 for Method 3 and 0.190 for Method 2. The improvement is greatest for parallel and pinnate basins. Using Method 2 for parallel basins, the K-S value is reduced by a third, while the value is halved for pinnate basins. For dendritic basins, almost no improvement is observed. Dendritic basins are expected to exhibit the highest degree of variability in their network structures because they develop without strong topographic or lithologic constraints. The K-S statistics for Method 1 are typically much lower than those of Method 2 (the average K-S statistic for Method 1 is 0.023). The only case where the A_{sc} distribution can be accurately estimated from the classification instead of the individual network is the pinnate classification (Fig. 4.5b).

4.2 Evaluation of Model Results

The synthetic UH method is tested by comparing the IUHs for four cases. Case 1 explicitly considers the individual cell slopes and the actual flow paths for each basin. This method is equivalent to an SDTT method and is considered the correct IUH for comparison purposes. Case 2 replaces the individual cell slopes with the estimates from S_h and the slope-area relationship, and it replaces the actual A_{sh} and A_{sc} distributions with the calibrated theoretical distributions. This case evaluates the assumptions required to construct a synthetic UH method. Case 3 estimates the parameters of the theoretical distributions based on the network classification. This is the classification-based synthetic UH method. Case 4 estimates the parameters of the theoretical distributions irrespective of the network classification. This case is analogous to traditional synthetic UH methods.

For this comparison, most of the parameters were set to constant values for all 50 basins to reduce confounding effects (Table 4.3). The selected Manning's roughness for the hillslopes n_h corresponds to short-grass prairie (McCuen et al., 2002). The roughness for channels n_c corresponds to a low-slope stream with weeds and stones or a mountain stream with cobbles and boulders (Chow, 1959). The fraction of area contributing flow r falls within the range for humid to arid climates (0.2 to 0.5) (Iacobellis and Fiorentino, 2000). The width-area coefficient d is a typical value (Montgomery and Gran, 2001). The b value varies between basins and is estimated from each basin's slope-area plot (as determined from each basin's DEM). For Cases 2 through 4, the average hillslope slope from the DEM of each basin was used for S_h .

Table 2.3 Model parameters used in the development of the instantaneous unit hydrographs (IUHs). Parameters that vary are determined from the digital elevation model (DEM) for each basin.

Parameter	Value	Units
Channel roughness (n_c)	0.05	$s/m^{1/3}$
Hillslope roughness (n_h)	0.15	$s/m^{1/3}$
Grid cell area (A)	Varies	m^2
Slope of hillslopes (S_h)	Varies	m/m
Slope-area factor (b)	Varies	$m^{-2\theta}$
Slope-area exponent (θ)	Varies	-
Width factor (d)	0.02	m^{1-2e}
Width exponent (e)	0.5	-
Fraction of area contributing (r)	0.3	m^2/m^2
Excess rainfall (E_i)	25.4	mm/hr

Figure 4.6 compares the IUHs from all four cases for the typical basin in each classification. The IUHs from Case 1 exhibit notable differences between the example basins from each classification. The IUH for the dendritic basin is negatively skewed, the IUH for the pinnate basin is positively skewed, and the IUHs for the other basins are nearly symmetrical. Comparing Figure 4.6 to the right column in Figure 4.2, one sees that the IUH shapes are almost identical to the A_{sc} distributions for the same basins. The A_{sc}

distributions play a much larger role than the A_{sh} distributions in determining the IUHs because 80% or more of the total travel time occurs in the channels.

When the slopes are approximated and the theoretical distribution is used (Case 2), the IUHs remain similar to Case 1, but the location fluctuations in the IUHs are lost (Fig. 4.6). For the pinnate and trellis basins, the IUHs for Case 2 also shift to the right. The travel times depend nonlinearly on slope, so using the average slope for a given contributing area is not equivalent to using the distribution of slopes for that contributing area. When the network type is used to estimate the IUH (Case 3), the IUH for the pinnate basin remains very close to Case 2 while the other basins deviate more. This result is consistent with the earlier results that showed the A_{sc} distributions are best estimated from the classification for the pinnate case. Case 4, which neglects the classification, has nearly zero skew and is a poor match for the IUHs from Case 1 for all basins shown.

Four metrics are used to quantify the difference in performance between the proposed synthetic UH method (Case 3) and the case that neglects classification (Case 4) for all 50 basins (Fig. 4.7). The first metric is the root mean squared error (RMSE) (Moriasi et al., 2007; Singh et al., 2005) where Case 1 is considered the observed IUH. The second metric is the Nash-Sutcliffe Coefficient of Efficiency (NSCE) (Nash and Sutcliffe, 1970). Because larger NSCE values indicate better performance (in contrast with the other metrics), Figure 4.7b instead shows 1 – NSCE so that lower values indicate better performance. The third metric is the absolute error in the IUH peak value, and the fourth metric is the absolute error in the time of the IUH peak. In Figure 4.7, the columns show the average performance for each classification, and black bars show the range of performance within each classification.

By most measures, considering the network classification provides little improvement in the estimated IUH. For time to peak, however, considering the classification improves the average performance for all classifications and reduces the range in performance for all classifications except trellis. This improvement occurs because the classification helps determine the skewness of the IUH as seen earlier. Considering the classification also provides an improvement in performance by all measures for the pinnate basins. Pinnate also has the lowest errors in comparison with other classifications. These results occur because the pinnate classification is an adequate substitute for the individual flow path network when estimating the A_{sh} and A_{sc} distributions.

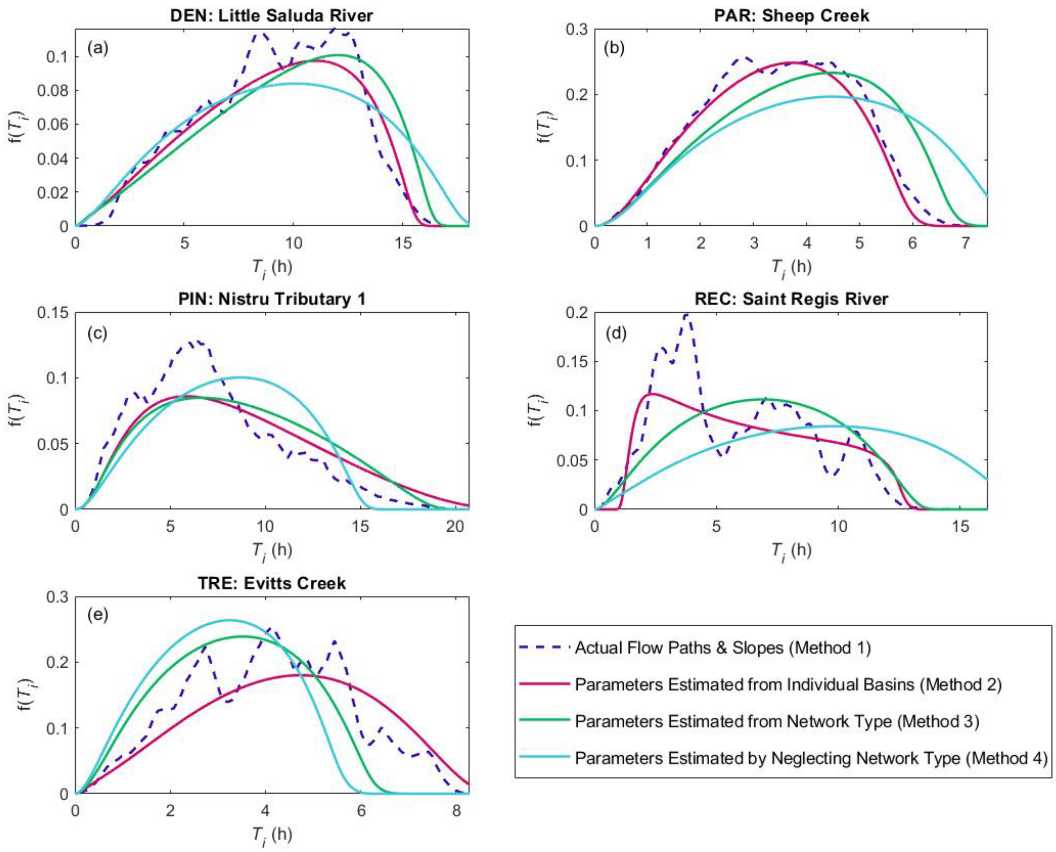

Figure 4.6 Instantaneous unit hydrographs (IUHs) estimated by the four methods described in the legend for an example basin in each classification.

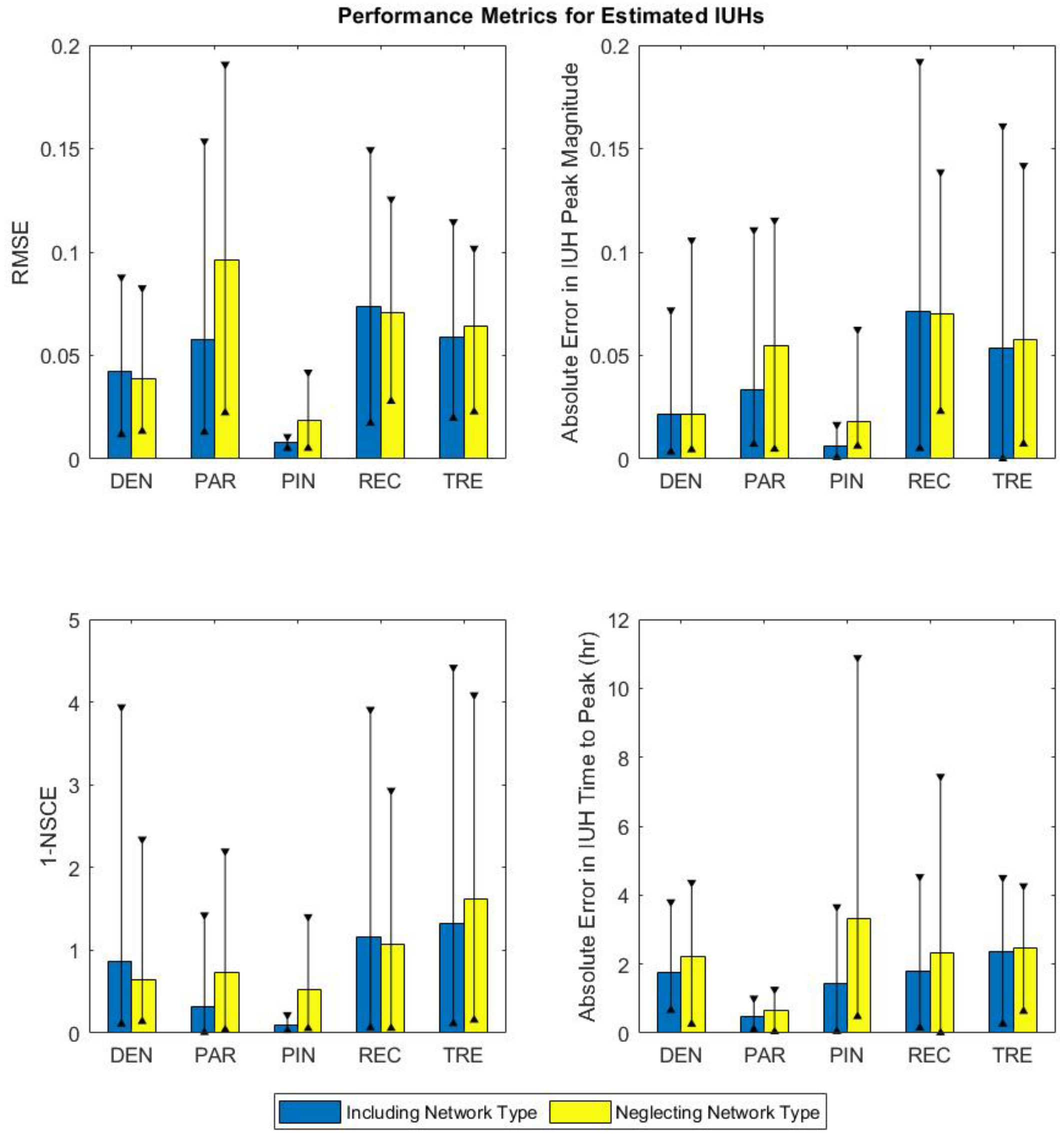

Figure 4.7 Performance metrics when the instantaneous unit hydrographs (IUHs) are estimated by either including or neglecting the network classification. Column heights indicate the average performance and black bars indicate the range of performance for each method.

5. CONCLUSIONS

This study developed and tested a nonlinear synthetic UH method that explicitly accounts for the network type (dendritic, parallel, pinnate, rectangular, and trellis). Within this approach, the network structure was isolated in two random variables, A_{sh} and A_{sc}, which characterize the flow paths for the hillslopes and channels, respectively. Based on this analysis, the following conclusions can be made:

1. Among the 24 theoretical distributions tested, the Johnson SB distribution best describes the observed distributions of A_{sh} and A_{sc}. For A_{sh}, the shape and location parameters of the gamma distribution are independent of the hillslope size $A_{h\max}$, but the scale parameter depends on $A_{h\max}$. Similarly, for A_{sc}, the shape and location parameters are independent of the basin size $A_{\max}$, but the scale parameter depends on $A_{\max}$.
2. The distributions of A_{sh} are significantly different between the five network classifications. Based on ANOVA and ANCOVA results, all 10 classification pairings have at least one distribution parameter that is significantly different. Because the classifications are determined from the channel network structure, this result suggests that the flow paths on the hillslopes (which determine A_{sh}) depend on the type of channel network into which they flow.
3. The distributions of A_{sc} are significantly different between the five classifications. From the ANOVA and ANCOVA results, 8 out of 10 classification pairings have at least one distribution parameter that is significantly different. The parameter that usually differs between classification pairs controls the skewness of the A_{sc} distribution. Dendritic and parallel basins have an abundance of locations that are distant from the outlet, which produces an abundance of large A_{sc} values and a negative skewness. In contrast, pinnate basins have more locations that are close to the outlet, which produces many small A_{sc} values and positive skewness. The other network types tend to have more symmetrical distributions for A_{sc}.
4. The A_{sh} distributions are more accurately estimated based on the network type than the A_{sc} distributions. The A_{sh} distributions exhibit relatively small differences between classifications but are relatively consistent within classifications, which allows accurate estimation of the distribution parameters. For A_{sc}, the differences within classifications are greater. Overall, the network type is most useful for estimating the A_{sc} distribution for parallel and pinnate networks, especially pinnate networks.
5. The IUHs from an SDTT method typically differ among the five network classifications. Much like the A_{sc} distributions, the IUHs of dendritic are negatively skewed, the IUHs for pinnate basins are positively skewed, and the IUHs for the other classifications are more symmetrical.
6. The proposed classification-based synthetic UH method, which estimates the A_{sh} and A_{sc} distributions based on the network classification, provides better estimates of the time to peak for the IUHs than a method that neglects classification. This improvement occurs because the time to peak is affected by the skewness of the A_{sh} and A_{sc} istributions, which are different among the classifications. However, other measures of performance, such as RMSE and NSCE, show little improvement when classification is considered. The exception is the pinnate classification, which shows noteworthy improvement in all measures when the classification is considered.

Overall, the results show that the five network classifications have differences in their IUHs and that considering network classification provides improved estimates of the IUHs. A classification-based synthetic UH has the potential to be used particularly for pinnate basins, but more testing is required. Independent validation should be performed by applying the method to basins that are not used in the model development. Testing on smaller basins is also needed. The results generated in this study considered large basins, but semi-distributed models often consider much smaller sub-basins. Further analyses of the interaction of channel network type and hillslope flow paths should also be performed. In particular, how does the role of the channel network type change as the active hillslope processes change? In addition, the assumption that a constant fraction of upstream area contributes flow at each time should be further analyzed. For example, a relationship between this fraction and basin size or grid cell location in the basin could be considered. The assumption that excess rainfall is produced uniformly across the basin could also be changed. Specifically, the differences in behavior between channel network types may differ if variable source areas produce the excess rainfall. Also, the IUHs from the proposed method were evaluated by comparing them with those from an SDTT model that explicitly represents the slopes and flow paths with the basin. Future research should evaluate the performance when the method is used to reproduce observed hydrographs. Such comparisons would allow testing of other assumptions in the method (e.g., the use of kinematic wave theory).

8. REFERENCES

Abu El-Nasr, A., Arnold, J.G., Feyen, J., and Berlamont, J., 2005. "Modelling the hydrology of a catchment using a distributed and a semi-distributed model." *Hydrol. Process*. 19, 573–587. doi:10.1002/hyp.5610

Argialas, D., Lyon, J., and Mintzer, O., 1988. "Quantitative description and classification of drainage patterns." *Photogramm. Eng. Remote Sensing* 54, 505–509.

Arnold, J.G., and Fohrer, N., 2005. "SWAT2000: Current capabilities and research opportunities in applied watershed modelling." *Hydrol. Process.* 19, 563–572. doi:10.1002/hyp.5611

Castelltort, S., Simpson, G., and Darrioulat, A., 2009. "Slope-control on the aspect ratio of river basins." *Terra* Nov. 21, 265–270. doi:10.1111/j.1365-3121.2009.00880.x

Chow, V.T., 1959. *Open-channel Hydraulics*, McGraw-Hill. ed. McGraw-Hill, New York.

Chow, V.T., Maidment, D.R., Mays, L.W., 1988. *Unit Hydrograph, in: Applied Hydrology.* McGraw-Hill Series in Water Resources and Environmental Engineering, pp. 201–233.

Clark, C.O., 1945. "Storage and the Unit Hydrograph." *Proc. Am. Soc. Civ. Eng* 69, 1333–1360.

Cohen, S., Willgoose, G., and Hancock, G., 2008. "A methodology for calculating the spatial distribution of the area-slope equation and the hypsometric integral within a catchment." *J. Geophys. Res. Earth Surf.* 113. doi:10.1029/2007JF000820

Cohen, Y., and Cohen, J.Y., 2008. *Analysis of Variance, in: Statistics and Data with R. John Wiley & Sons, Ltd,* Chichester, UK, pp. 463–509. doi:10.1002/9780470721896.ch15

D'Agostino, R.B., and Stephens, M.A. (Eds.), 1986. *Goodness-of-Fit Techniques.* Marcel Dekker, Inc., New York, NY. doi:10.2307/1165059

Du, J., Xie, H., Hu, Y., Xu, Y., and Xu, C.Y., 2009. "Development and testing of a new storm runoff routing approach based on time variant spatially distributed travel time method." *J. Hydrol.* 369, 44–54. doi:10.1016/j.jhydrol.2009.02.033

Dunne, T., and Black, R.D., 1970. "Partial Area Contributions to Storm Runoff in a Small New England Watershed." *Water Resour. Res.* 6, 1296–1311. doi:10.1029/WR006i005p01296

Feldman, A.D., 2000. *Hydrologic modeling system HEC-HMS*, U.S. Army Corps of Engineers Technical Reference Manual. doi:CDP-74B

Flint, J.J., 1974. "Stream gradient as a function of order, magnitude, and discharge." *Water Resour. Res.* 10, 969–973. doi:10.1029/WR010i005p00969

George, F., and Ramachandran, K.M., 2011. "Estimation of Parameters of Johnson's System of Distributions." *J. Mod. Appl. Stat. Methods* 10, 494–504. doi:10.22237/jmasm/1320120480

Gilbert, G.K., 1909. "The Convexity of Hilltops." *J. Geol.* 17, 344–350. doi:10.1086/621620

Gironás, J., Niemann, J.D., Roesner, L.A., Rodriguez, F., and Andrieu, H., 2009. "A morpho-climatic instantaneous unit hydrograph model for urban catchments based on the kinematic wave approximation." *J. Hydrol.* 377, 317–334. doi:10.1016/j.jhydrol.2009.08.030

Gupta, V.K., and Waymire, E., 1983. "On the formulation of an analytical approach to hydrologic response and similarity at the basin scale." *J. Hydrol.* 65, 95–123. doi:10.1016/0022-1694(83)90212-3

Gupta, V.K., Waymire, E., and Wang, C.T., 1980. "A representation of an instantaneous unit hydrograph from geomorphology." *Water Resour. Res.* 16, 855–862. doi:10.1029/WR016i005p00855

Hack, J.T., 1957. "Studies of longitudinal stream profiles in Virginia and Maryland," Geological Survey. Professional Paper 294-B.

Hadipriono, F.C., Lyon, J.G., and Li, T., 1990. "The development of a knowledge based expert system for analysis of drainage patterns." *Photogramm. Eng. Remote Sens.* 56, 905–909.

Haghnegahdar, A., Tolson, B.A., Craig, J.R., and Paya, K.T., 2015. "Assessing the performance of a semi-distributed hydrological model under various watershed discretization schemes." *Hydrol. Process.* 29, 4018–4031. doi:10.1002/hyp.10550

Howard, A.D., 1967. "Drainage Analysis in Geologic Interpretation: A Summation." *Am. Assoc. Pet. Geol. Bull.* 51, 2246–2259. doi:10.1306/5D25C26D-16C1-11D7-8645000102C1865D

Iacobellis, V., and Fiorentino, M., 2000. "Derived distribution of floods based on the concept of partial area coverage with a climatic appeal." *Water Resour. Res.* 36, 469–482. doi:0042-1397/00/1999WR900287

Ichoku, C., and Chorowicz, J., 1994. "A numerical approach to the analysis and classification of channel network patterns types." *Water Resour. Res*. 30, 161–174.

Ijjasz-Vasquez, E.J., and Bras, R.L., 1995. "Scaling regimes of local slope versus contributing area in digital elevation models." *Geomorphology* 12, 299–311. doi:10.1016/0169-555X(95)00012-T

Jogesh Babu, G., and Rao, C.R., 2004. "Goodness-of-fit tests when parameters are estimated." *Indian J. Stat.* 66, 63–74.

Jung, K., Marpu, P.R., and Ouarda, T.B.M.J., 2017. "Impact of river network type on the time of concentration." *Arab. J. Geosci.* 10, 546. doi:10.1007/s12517-017-3323-3

Jung, K., Niemann, J.D., and Huang, X., 2011. "Under what conditions do parallel river networks occur?" *Geomorphology* 132, 260–271. doi:10.1016/j.geomorph.2011.05.014

Kottegoda, N.T., 1987. "Fitting Johnson SB Curve by the Method of Maximum Likelihood to Annual Maximum Daily Rainfalls." *Water Resour. Res.* 23, 728–732.

Kull, D.W., and Feldman, A.D., 1998. "Evolution of Clark's Unit Graph Method to Spatially Distributed Runoff." *J. Hydrol. Eng.* 3, 9–19. doi:10.1061/(ASCE)1084-0699(1998)3:1(9)

Lee, K.T., Chen, N.-C., and Chung, Y.-R., 2008. "Derivation of variable IUH corresponding to time-varying rainfall intensity during storms." *Hydrol. Sci. J.* 53, 323–337. doi:10.1623/hysj.53.2.323

Lee, K.T., and Yen, B.C., 1997. "Geomorphology and Kinematic-Wave–Based Hydrograph Derivation." *J. Hydraul. Eng.* 123, 73–80. doi:10.1061/(Asce)0733-9429(1997)123:1(73)

Leopold, L.B., and Maddock, T.J., 1953. "The Hydraulic Geometry of Stream Channels and Some Physiographic Implications," Geological Survey Professional Paper 252. doi:10.1016/S0169-555X(96)00028-1

Maidment, D.R., 1993. *GIS and hydrological modeling, Environmental Modeling within GIS.* Oxford: University Press, New York, NY.

Maxwell, S., and Delaney, H., 2004. *Designing experiments and analyzing data: A model comparison perspective, Briefings in functional genomics proteomics.* Taylor & Fancis Group, LLC., New York, NY. doi:10.1002/sim.4780100917

McCuen, R.H., Johnson, P.A., and Ragan, R.M., 2002. *Highway Hydrology: Hydraulic Design Series No. 2*. Arlington, VA.

Mejía, A.I., and Niemann, J.D., 2008. "Identification and characterization of dendritic, parallel, pinnate, rectangular, and trellis networks based on deviations from planform self-similarity." *J. Geophys. Res.* 113, F02015. doi:10.1029/2007JF000781

Melesse, A.M., and Graham, W.D., 2004. "Storm Runoff Prediction Based on a Spatially Distributed Travel Time Method Utilizing Remote Sensing and GIS." *J. Am. Water Resour. Assoc.* 9007, 863–879.

Montgomery, D.R., 2001. "Slope distributions, threshold hillslopes, and steady-state topography." *Am. J. Sci.* 301, 432–454. doi:10.2475/ajs.301.4-5.432

Montgomery, D.R., and Gran, K.B., 2001. "Downstream variations in the width of bedrock channels." *Water Resour. Res.* 37, 1841–1846.

Moriasi, D.N., Arnold, J.G., Van Liew, M.W., Bingner, R.L., Harmel, R.D., and Veith, T.L., 2007. "Model Evaluation Guidelines for Systematic Quantification of Accuracy in Watershed Simulations." *Trans. ASABE* 50, 885–900. doi:10.13031/2013.23153

Muzik, I., 1996. "Flood modelling with GIS-derived distributed unit hydrographs." *Hydrol. Process.* 10, 1401–1409. doi:10.1002/(SICI)1099-1085(199610)10:10<1401::AID-HYP469>3.0.CO;2-3

Nash, J.E., and Sutcliffe, J. V., 1970. "River flow forecasting through conceptual models part I - A discussion of principles." *J. Hydrol.* 10, 282–290. doi:10.1016/0022-1694(70)90255-6

Niemann, J.D., Bras, R.L., Veneziano, D., and Rinaldo, A., 2001. "Impacts of surface elevation on the growth and scaling properties of simulated river networks." *Geomorphology* 40, 37–55. doi:10.1016/S0169-555X(01)00036-8

NRCS, 2007. *Hydrographs, in: National Engineering Handbook*. U.S. Department of Agriculture, Washington, D.C., p. 16.

O'Callaghan, J.F., and Mark, D.M., 1984. "The extraction of drainage networks from digital elevation data." *Comput. Vision, Graph. Image Process.* 28, 323–344. doi:10.1016/S0734-189X(84)80011-0

Parvis, M., 1950. "Drainage pattern significance in airphoto identification of soils and bedrocks." *Photogramm. Eng.* 16, 375–409.

Peters, J.C., and Easton, D.J., 1996. "Runoff Simulation Using Radar Rainfall Data." *J. Am. Water Resour. Assoc.* 32, 753–760. doi:10.1111/j.1752-1688.1996.tb03472.x

Phillips, L.F., and Schumm, S.A., 1987. "Effect of regional slope on drainage networks." *Geology.* doi:10.1130/0091-7613(1987)15<813:EORSOD>2.0.CO

Reed, S., Koren, V., Smith, M., Zhang, Z., Moreda, F., and Seo, D.J., 2004. "Overall distributed model intercomparison project results." *Journal of Hydrology*. pp. 27–60. doi:10.1016/j.jhydrol.2004.03.031

Rinaldo, A., Vogel, G.K., Rigon, R., and Rodriguez-Iturbe, I., 1995. "Can One Gauge the Shape of a Basin?" *Water Resour. Res.* 31, 1119–1127. doi:10.1029/94WR03290

Robinson, J.J.S., and Sivapalan, M., 1996. "Instantaneous Response Functions of Overland Flow and Subsurface Stormflow for Catchment Models." *Hydrol. Process.* 10, 845–862. doi:10.1002/(SICI)1099-1085(199606)10:6<845::AID-HYP375>3.0.CO;2-7

Rodríguez-Iturbe, I., and Valdes, J.B., 1979. "The Geomorpholic Structure of Hydrologic Response." *Water Resour. Res.* 15, 1409–1420. doi:10.1029/WR015i006p01409

Rodríguez-Iturbe, I., González-Sanabria, M., and Bras, R.L., 1982. "A geomorphoclimatic theory of the instantaneous unit hydrograph." *Water Resour. Res.* 18, 877–886. doi:10.1029/WR018i004p00877

Roering, J.J., Kirchner, J.W., and Dietrich, W.E., 2001. "Hillslope evolution by nonlinear, slope-dependent transport: Steady state morphology and equilibrium adjustment timescales." *J. Geophys. Res.* 106, 26787. doi:10.1029/2001JB900018

Saghafian, B., Julien, P.Y., and Rajaie, H., 2002. "Runoff hydrograph simulation based on time variable isochrone technique." *J. Hydrol.* 261, 193–203. doi:10.1016/S0022-1694(02)00007-0

SCS, 1972. SCS *National Engineering Handbook. Section 4, Hydrology,* in: National Engineering Handbook.

Singh, J., Knapp, H.V., Arnold, J.G., and Demissie, M., 2005. "Hydrological modeling of the Iroquois River watershed using HSPF and SWAT." *JAWRA J. Am. Water Resour. Assoc.* 41, 343–360. doi:10.1111/j.1752-1688.2005.tb03740.x

Singh, P.K., Mishra, S.K., and Jain, M.K., 2014. "A review of the synthetic unit hydrograph: from the empirical UH to advanced geomorphological methods." *Hydrol. Sci. J.* 59, 239–261. doi:10.1080/02626667.2013.870664

Singh, V.P., 1998. *Gamma Distribution, in: Entropy-Based Parameter Estimation in Hydrology.* Springer, Dordrecht, pp. 202–203. doi:10.1007/978-94-017-1431-0

Sklar, L., Dietrich, and W.E., 2013. "River Longitudinal Profiles and Bedrock Incision Models: Stream Power and the Influence of Sediment Supply, in: Rivers Over Rock: Fluvial Processes in Bedrock Channels." *American Geophysical Union,* p. 237. doi:10.1029/GM107p0237

Snyder, F.F., 1938. "Synthetic unit-graphs." *Trans. Am. Geophys. Union* 19, 447–454. doi:10.1029/TR019i001p00447

Snyder, N.P., Whipple, K.X., Tucker, G.E., and Merritts, D.J., 2003. "Importance of a stochastic distribution of floods and erosion thresholds in the bedrock river incision problem." *J. Geophys. Res.* 108. doi:10.1029/2001JB001655

Strahler, A.N., 1957. "Quantitative analysis of watershed geomorphology." *Eos, Trans. Am. Geophys. Union* 38, 913–920. doi:10.1029/TR038i006p00913

Tarboton, D.G., 2003. "Terrain Analysis Using Digital Elevation Models (TauDEM, ver. 5.3.5)," in: 23rd ESRI International Users Conference.

Tarboton, D.G., Bras, R.L., and Rodriguez-Iturbe, I., 1991. "On the extraction of channel networks from digital elevation data." *Hydrol. Process.* 5, 81–100. doi:10.1002/hyp.3360050107

Tarboton, D.G., Bras, R.L., and Rodriguez-Iturbe, I., 1989. "Scaling and elevation in river networks." *Water Resour. Res.* 25, 2037–2051. doi:10.1029/WR025i009p02037

Taylor, J., 1997. *Introduction to Error Analysis, the Study of Uncertainties in Physical Measurements,* 2nd Edition, University Science Books. Sausalito, CA.

Tucker, G.E., and Bras, R.L., 1998. "Hillslope processes, drainage density, and landscape morphology." *Water Resour. Res.* 34, 2751–2764. doi:10.1029/98WR01474

Tucker, G.E., Catani, F., Rinaldo, A., and Bras, R.L., 2001. "Statistical analysis of drainage density from digital terrain data." *Geomorphology* 36, 187–202. doi:10.1016/S0169-555X(00)00056-8

van der Tak, L.D., and Bras, R.L., 1990. "Incorporating hillslope effects into the geomorphologic instantaneous unit hydrograph." *Water Resour. Res.* 26, 2393–2400. doi:10.1029/WR026i010p02393

Weber, M.D., Leemis, L.M., and Kincaid, R.K., 2006. "Minimum Kolmogorov-Smirnov test statistic parameter estimates." *J. Stat. Comput. Simul.* 76, 195–206. doi:10.1080/00949650412331321098

Willgoose, G., Bras, R.L., and Rodriguez-Iturbe, I., 1991. "A physical explanation of an observed link area-slope relationship." *Water Resour. Res.* 27, 1697–1702. doi:10.1029/91WR00937

Wolman, M.G., 1955. The Natural Channel of Brandywine Creek Pennsylvania, Geological Survey Professional Paper 271.

Wong, T.S.W., 2001. "Formulas for time of travel in channel with upstream inflow." *J. Hydrol. Eng.* 6, 416–422.

Wong, T.S.W., 1995. "Time of concentration formulae for planes with upstream inflow." *Hydrol. Sci. J.* 40, 663–666. doi:10.1080/02626669509491451

Xia, J., Wang, G., Tan, G., Ye, A., and Huang, G.H., 2005. "Development of distributed time-variant gain model for nonlinear hydrological systems." *Sci. China Ser. D* 48, 713–723. doi:10.1360/03yd0183

Zernitz, E.R., 1932. "Drainage Patterns and Their Significance." *J. Geol.* 40, 498–521. doi:10.1086/623976

Zoch, R.T., 1934. "On the relation between rainfall and stream flow." *Mon. Weather Rev.* 62, 315–322. doi:10.1175/1520-0493(1934)62<315:otrbra>2.0.co;2

Zuazo, V., Gironás, J., and Niemann, J.D., 2014. "Assessing the impact of travel time formulations on the performance of spatially distributed travel time methods applied to hillslopes." *J. Hydrol.* 519, 1315–1327. doi:10.1016/j.jhydrol.2014.09.035